

# Length Scales and Power Laws in the Two-Dimensional Forest-Fire Model

A. Honecker and I. Peschel

*Fachbereich Physik, Freie Universität Berlin,  
Arnimallee 14, D-14195 Berlin, Germany*

## Abstract

We re-examine a two-dimensional forest-fire model via Monte-Carlo simulations and show the existence of two length scales with different critical exponents associated with clusters and with the usual two-point correlation function of trees. We check resp. improve previously obtained values for other critical exponents and perform a first investigation of the critical behaviour of the slowest relaxational mode. We also investigate the possibility of describing the critical point in terms of a distribution of the global density. We find that some qualitative features such as a temporal oscillation and a power law of the cluster-size distribution can nicely be obtained from such a model that discards the spatial structure.

---

e-mail:

honecker@physik.fu-berlin.de

peschel@aster.physik.fu-berlin.de

# 1. Introduction

---

Dynamical systems that are naturally close to or on their critical point have been proposed as an explanation of the appearance of power laws in nature [1, 2]. This ‘self-organized criticality’ still consists to a large extent in the study of toy models and has many open or controversial questions. The lattice models can be grouped at least into three classes. A first class contains models with a local conservation law like the famous sandpile-model [1, 2]. Recent experiments on piles of rice [3] partially confirm the general theoretical predictions by exhibiting power laws, but also show that the existence of power laws in real systems depends on microscopic details such as the aspect ratio of grains of rice. Models of evolution [4, 5] are one example in a second class where the dynamics is specified in terms of a globally selected extremal site. This extremal dynamics can be used to obtain some general statements for the complete class of models [6]. The forest-fire model is a member of a third class of models that have parameters which can be tuned close to the critical point in a natural manner, but unlike in the two previous classes cannot be entirely discarded. The precise version that we study in this paper has first been introduced in a short note [7] and arises as a certain limit of the more general model proposed later independently in [8].

The two-dimensional forest-fire model has been already discussed very controversially, mainly on the basis of Monte-Carlo simulations where usually the accuracy of the predictions was the issue. An originally proposed version [9] did not show the desired critical behaviour [10, 11], and it was necessary to introduce lightnings [8]. Subsequently, Monte-Carlo simulations have several times lead to values for the critical exponents which had to be corrected later on [8, 12, 13, 14]. Here we add to this discussion by re-examining some of the quantities investigated only in one of the earlier works [12]. We were motivated by a study of the one-dimensional case [15] where we had discovered the existence of two different length scales. The analogous question in two dimensions has been addressed in [12], but there it seemed that the two scales are proportional to each other. Here, we present more accurate simulations that demonstrate these two length scales to be different also in two dimensions. As by-products we also check or improve estimates for other exponents (see in particular [14]). A final subject is the approach to equilibrium which seems not to have been addressed in a similar way before. In a second part, we try to discard the spatial structure and introduce a global model similar to the one of [15] for one dimension. On the one hand, some of the qualitative features of the stationary state at the critical point (e.g. the power law of the cluster-size distribution) can nicely be described by such a global model. On the other hand, there are discrepancies in quantitative details and the range of such a simplified model is very limited in comparison to the full model. We believe that this is an important point, e.g. because it has been suggested in [16] that power laws in nature might arise from a global (‘coherent’) driving that does not see any spatial structure. Our findings here and in the one-dimensional case [15] demonstrate that the full model is not only different from but also richer than the simplified model. This is analogous to the result of [17] that versions of certain models of evolution with and without spatial structure lead to different results (at least if examined closely).

We would like to conclude these introductory remarks with a definition of the model before we proceed with a presentation of our simulation results in the next Section. The forest-fire model is defined on a cubic lattice in  $d$  dimensions. Any site can have two states: It can either be empty or it can be occupied by a tree. The dynamics of the model is specified

by the following update rules (following [7, 12, 13, 14]<sup>1)</sup>): In each Monte-Carlo step first choose an arbitrary site of the lattice.

- a) If it is empty, grow a tree there with probability  $p$ .
- b) If it is occupied by a tree, delete the entire geometric cluster of trees connected to it with probability  $f$ .

This corresponds to a lightning stroke with subsequent spreading of the fire.

A rescaling of the probabilities  $p$  and  $f$  just amounts to a rescaling of the time scale, and in particular leaves the stationary state invariant. We exploit this to set  $p = 1$ . There is a critical point at  $f/p = 0$ , but the parameter  $f/p$  is relevant and it is not possible to consider the forest-fire model precisely at this critical point (compare [18]).

Due to the selection of a single site, the time evolution measured in terms of Monte-Carlo steps scales linearly with the volume of the system. Therefore, we introduce a second ‘global’ time scale a unit of which is defined by the number of Monte-Carlo steps needed in order to visit each site in average precisely once. In this way one can directly compare with the times appearing in a simulation with parallel dynamics or with the time appearing in the definition of the master equation (which has been used in [15]).

## 2. Simulation results in two dimensions

---

In the following we consider the two-dimensional version of the forest-fire model on a quadratic lattice with periodic boundary conditions. The linear size of the lattice will be denoted by  $L$ . So the volume  $V$  is given by  $V = L^2$ , and a unit of global time consists of  $L^2$  Monte-Carlo steps.

In order to do the simulation efficiently also for large systems and small  $f/p$  one has to be careful and use e.g. bitmapping technologies. For details on the implementation compare the WWW page [19].

We have investigated mainly systems of linear size  $L = 16384$  and parameter values  $10^{-2} \geq f/p \geq 10^{-4}$ . For a simulation, one random initial condition with density  $\rho = 1/2$  was chosen. In order to equilibrate the system, it was left to evolving freely for at least 15 global time units. This equilibration time was increased to 25 global time units for  $f/p \leq 3 \cdot 10^{-4}$  and to 35 global time units for  $f/p = 1 \cdot 10^{-4}$ . After this, the system was iterated further for another 60 to 90 global time units (120 units for  $f/p = 3 \cdot 10^{-4}$ ). During this period, measurements were made as global averages at intervals of usually one global time unit (for the density 200 times more frequently). This amounts to at least  $60L^2$  measurements for each quantity of interest. Note that we use only a single run.

### 2.1 Correlation functions

---

Let us first discuss the simulation results for the usual tree correlation function  $\langle T(\vec{x})T(\vec{x} + \vec{y}) \rangle$ . We have only investigated displacements  $\vec{y}$  along the vertical axis (which can be treated particularly efficiently using bitmaps). The data resulting from the simulation can nicely be fitted by

$$C(y) := \langle T(\vec{x})T(\vec{x} + y\vec{e}_2) \rangle - \langle T(\vec{x}) \rangle^2 = ae^{-y/\xi} \quad (2.1)$$

---

<sup>1)</sup> To be precise, the simulations in [13, 14] have been performed according to slightly different rules, because they aimed at investigating only quantities associated with clusters.

in a suitable interval  $y_{\min} \leq y \leq y_{\max}$ . The parameters  $a$  and  $\xi$  were estimated by taking the logarithm of the r.h.s. of (2.1) and then performing a linear regression for  $y_{\min} \leq y \leq y_{\max}$ . These bounds are chosen such that the approximation (2.1) by a single exponential function is good. The lower cutoff can be chosen small ( $y_{\min} \approx 20$ ) independent of  $f/p$ . An upper cutoff  $y_{\max}$  has to be imposed at distances of 4 to 7 times the correlation length  $\xi$  because then statistical errors become large.

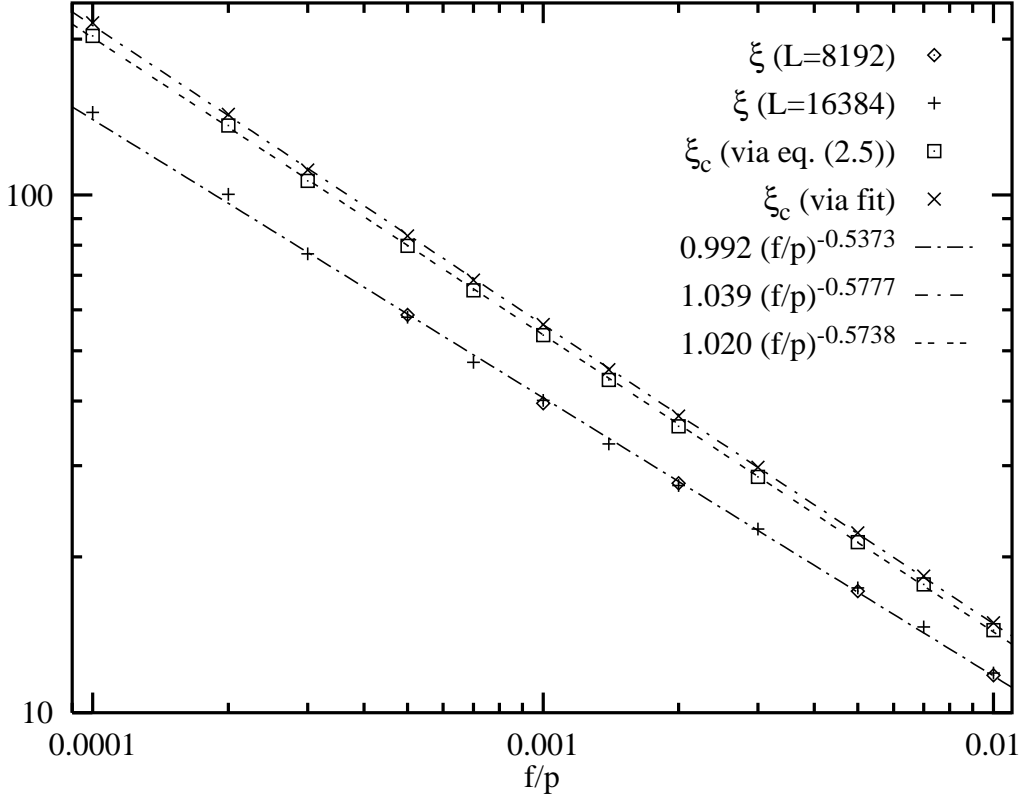


**Fig. 1:** The two correlation lengths  $\xi$  and  $\xi_c$ . For  $\xi_c$  all estimates are on lattices with  $L = 16384$  and the different symbols correspond to different ways of treating the data.

Fig. 1 shows the results for  $\xi$  obtained in this manner on lattices with  $L = 8192$  (diamonds) and  $L = 16384$  (crosses). One observes that they are in good agreement with the form

$$\xi \sim \left( \frac{f}{p} \right)^{-\nu_T}. \quad (2.2)$$

Performing linear regression fits on a doubly logarithmic scale one finds

$$\nu_T = 0.537 \pm 0.004. \quad (2.3)$$

This is close to the result  $\nu_T = 0.56$  found in [12]. The values for  $\xi$  are very stable across simulations with a different amount of data as one can see in Fig. 1. So, the result (2.3) for  $\nu_T$  and its error bound are reliable.

The estimates for the normalization constant  $a$  in (2.1) are compatible with a value  $a = 0.030 \pm 0.001$  independent of  $f/p$ . So, in the limit  $f/p \rightarrow 0$  the two-point function seems to

tend to  $\langle T(\vec{x}) \rangle^2 + a$  for  $y \gtrsim 100$ . In terms of the alternative ansatz  $C(y) = ay^{-\eta_{\text{occ}}}e^{-y/\xi}$  used in [12] this corresponds to  $\eta_{\text{occ}} = 0$ , while the result found there was  $\eta_{\text{occ}} = 0.120 \pm 0.015$ . We have also looked into the possibility of a power-law correction using our data for  $L = 16384$  and  $f/p \leq 3 \cdot 10^{-4}$ . With the estimates for  $\xi$  shown in Fig. 1 one finds that  $e^{y/\xi}C(y) \sim y^{-0.11}$  for  $y \leq 20$ , i.e. for small  $y$  there is indeed a power-law correction with an exponent that is consistent with [12]. On the other hand, for  $50 \leq y \leq 4\xi$ , the function  $e^{y/\xi}C(y)$  is flat – its smallest values are around 0.27 and its maximal values around 0.31. This clearly contradicts a power-law correction with  $\eta_{\text{occ}} \approx 0.11$  in the large-distance asymptotics. Thus, for the large-distance behaviour  $\eta_{\text{occ}} = 0$  seems to be correct, while the power-law correction observed in [12] applies to small distances.

We now look at a second quantity, namely the ‘connected correlation function’  $\langle T(\vec{x})T(\vec{x} + \vec{y}) \rangle_c$  describing the probability to find two trees at positions  $\vec{x}$  and  $\vec{x} + \vec{y}$  *inside the same cluster*. This quantity is usually referred to as *the* two-point function in the context of self-organized criticality and often is also the only correlation function that is investigated. We demonstrated in one spatial dimension [15] that the length scales associated to this correlation function and  $C(y)$  have different critical exponents while [12] suggested that in two dimensions length scales associated to different quantities are equivalent. This latter suggestion was based on simulations with lattice sizes up to  $512 \times 512$  and  $f/p \gtrsim 5 \cdot 10^{-4}$ . One of the main aims of the simulations presented here is to check if different length scales can be exhibited also in two dimensions after sufficiently improving the accuracy. As before, we restrict to displacements  $\vec{y}$  along the vertical axis, i.e. we consider

$$K(y) := \langle T(\vec{x})T(\vec{x} + y\vec{e}_2) \rangle_c. \quad (2.4)$$

This quantity can be determined in the same run as the two-point function  $\langle T(\vec{x})T(\vec{x} + \vec{y}) \rangle$ , but it involves the additional effort of determining all clusters present in the system.

Following [14] we associate a correlation length  $\xi_c$  to the second moment of  $K(y)$  via

$$\xi_c^2 := \frac{\sum_{y=1}^{\infty} y^2 K(y)}{\sum_{y=1}^{\infty} K(y)}. \quad (2.5)$$

The squares in Fig. 1 show values of  $\xi_c$  extracted from simulations with  $L = 16384$  using this definition. One sees that these values are consistent with

$$\xi_c \sim \left( \frac{f}{p} \right)^{-\nu}. \quad (2.6)$$

and a (preliminary) value of

$$\nu = 0.5738 \pm 0.0013. \quad (2.7)$$

This agrees roughly with the value  $\nu = 0.60$  found in [12], and also with the more accurate result in [14] which, including error bounds, is given by  $\nu = 0.580 \pm 0.003$  [20]. It should be noted that the lower bound  $y = 1$  in (2.5) is crucial. Starting the summation instead e.g. at  $y = 10$ , one finds  $\xi_c \approx 24$  at  $f/p = 10^{-2}$  and  $\xi_c \approx 219$  for  $f/p = 10^{-4}$ . This in turn would make the value for  $\nu$  smaller. We will argue soon that the start of summation  $y = 1$  is indeed the correct choice, but the impact of a modification here could give rise to a slightly larger error than the  $1\sigma$  interval for the fit given in (2.7).

We now proceed with a more detailed discussion of the form of  $K(y)$  which will also justify the definition (2.5). Eq. (2.5) is based on the following expected form of  $K(y)$ :

$$K(y) = a_c y^{-\eta} e^{-y/\xi_c}. \quad (2.8)$$

In particular, if  $e^{-y/\xi_c} K(y)$  agrees well with a power law, the determination of  $\xi_c$  via (2.5) is justified. Using the values of  $\xi_c$  given by the boxes in Fig. 1 one finds that  $e^{-y/\xi_c} K(y)$  does indeed agree well with  $a_c y^{-\eta}$  for  $y$  between 1 and several times  $\xi_c$ <sup>2)</sup>. The crosses in Fig. 2 show these estimates for  $\eta$ . To determine the value of  $\eta$  in the limit  $f/p \rightarrow 0$  we make a scaling ansatz  $\eta(f/p) = \eta + \bar{a} (f/p)^{\bar{b}}$ . A least-squares fit gives the dotted line in Fig. 2. One finds a critical  $\eta = 0.374 \pm 0.011$ .

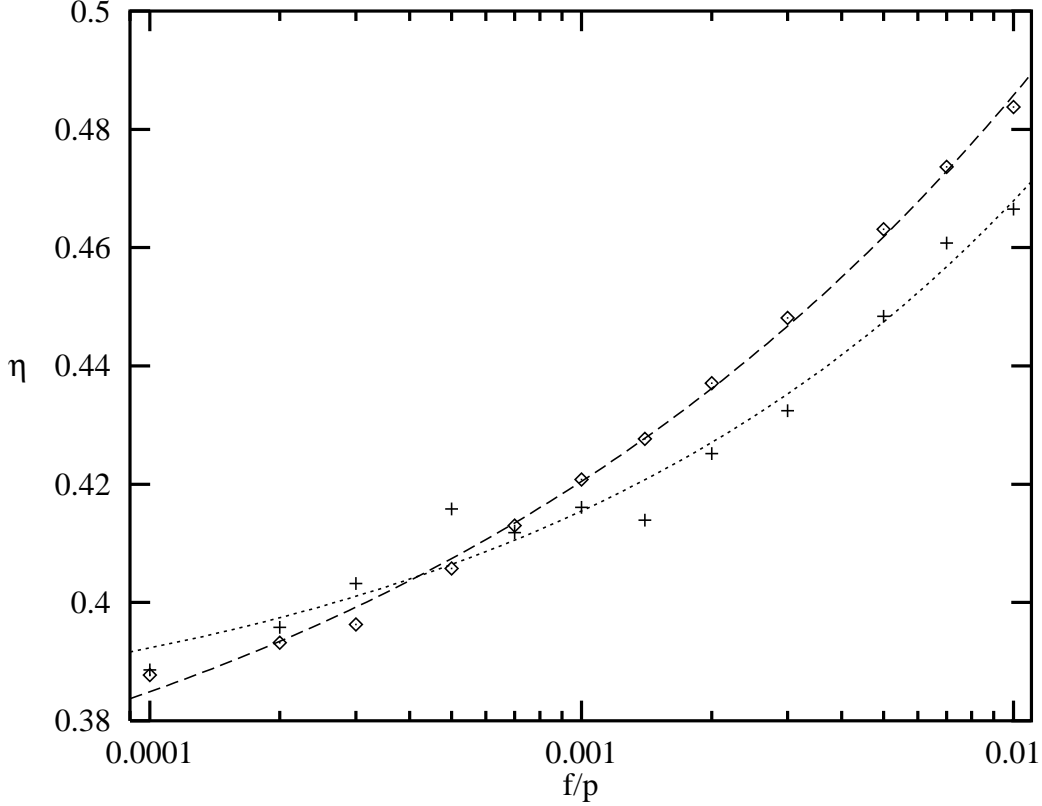


**Fig. 2:** Values for the exponent  $\eta$  obtained in two different ways (crosses and diamonds) and scaling fits (lines).

Alternatively, one can fit all three parameters in (2.8) directly from the data. The values for  $\eta$  obtained with this approach are shown in Fig. 2 by diamonds. A scaling analysis (the line with long dashes in Fig. 2) yields a critical  $\eta = 0.342 \pm 0.008$ . Comparing this with the value found earlier, one finds a small disagreement. So, the error bounds of these two estimates for the critical  $\eta$  may be a little too optimistic because they do not include systematic errors. In order to be careful we give a final result that includes both estimates for  $\eta$  and the two error ranges:

$$\eta = 0.36 \pm 0.03. \quad (2.9)$$

<sup>2)</sup> The values of  $a_c$  are all compatible with the  $f/p$ -independent value  $a_c = 0.20 \pm 0.01$ . Therefore, at the critical point the power law  $K(y) = a_c y^{-\eta}$  is expected to be valid for all  $y$ .

This is compatible with the result  $\eta = 0.411 \pm 0.02$  of [12] (although the error estimate of [12] seems a little too optimistic, possibly because it does not take systematic errors into account). One also obtains different estimates for  $\xi_c$  from the same fits that gave the alternative values for  $\eta$ . These values are shown in Fig. 1 by the diagonal crosses. One sees that they are again compatible with the form (2.6), and obtains an alternative estimate for the associated critical exponent:  $\nu = 0.5777 \pm 0.0013$ . There is a minor difference between this value and the earlier estimate (2.7) indicating that we have indeed neglected systematic errors. Therefore we give a final result

$$\nu = 0.576 \pm 0.003 \quad (2.10)$$

which includes the two direct estimates and their error bound. This final result is in excellent agreement with [14].

Comparing (2.10) with (2.3), we see that  $\nu \neq \nu_T$ , so that  $\xi_c$  and  $\xi$  are basically different lengths. A difference  $\nu - \nu_T \approx 0.4$  was already observed in [12], but attributed to numerical errors because it was unexpected.

It should be mentioned that our results (2.9) and (2.10) for  $\eta$  and  $\nu$  do not satisfy the scaling relation  $2 - \eta = 1/\nu$  [12]. We can only speculate about the reason for the disagreement. For example, in the derivation of this scaling relation one assumes that  $\eta$  and  $\nu$  do not depend on the direction of the displacement vector  $\vec{y}$ , and we have not checked whether this is indeed true. Another possibility is that we have still overlooked systematic errors. Inserting  $\nu$  (which is the more reliable value) according to (2.10) into the scaling relation  $2 - \eta = 1/\nu$  yields  $\eta \approx 0.28$  which is possible if our error estimate in (2.9) is by a factor of about 3 too small.

## 2.2 Cluster-size distribution

---

The distribution  $n(s)$  of clusters with size  $s$  arises as a by-product of the determination of  $K(y)$  during the simulations. We extract an exponent  $\tau$  from it following the lines described in detail in [12, 13]. One introduces the quantity  $P(s) = \sum_{s' > s} s' n(s')$ . Assuming that it behaves as  $P(s) = \alpha s^{2-\tau} e^{-s/s_{\max}}$ , one can use three-parameter fits to obtain estimates for  $\tau$  and  $s_{\max}$ . Extrapolation of the values obtained in this manner from the simulations with  $L = 16384$  yields  $\tau = 2.1595 \pm 0.0045$  for  $f/p \rightarrow 0$ . The values of  $\tau$  for  $f/p > 0$  approach this limiting value from above. An alternative way to extract a value of  $\tau$  is to look directly at  $n(s)$  and assume that  $n(s) \sim s^{-\tau}$  for intermediate  $s$ . Applying this second method to the same data and to some results for  $L = 8192$  we obtain the estimate  $\tau = 2.159 \pm 0.006$  at the critical point. This limit is now approached from below and is in excellent agreement with the one obtained before. To be on the safe side we retain the value with the larger error bound as the final result:

$$\tau = 2.159 \pm 0.006. \quad (2.11)$$

This value agrees within error bounds with most previous results [12, 21, 13, 14], but our error bound is considerably smaller than in most of them.

When one extracts estimates for  $\tau$  from  $P(s)$  one also obtains estimates for  $s_{\max}$ . These values are in good agreement with the form  $s_{\max} \sim (f/p)^{-\lambda}$  with  $\lambda = 1.171 \pm 0.004$ . To check the validity of our error estimate we can use the scaling relation  $\lambda = 1/(3 - \tau)$  [14].

After inserting (2.11) one finds the prediction  $\lambda = 1.189 \pm 0.008$ . This prediction agrees roughly with the direct estimate. However, there is a small discrepancy indicating that the estimate

$$\lambda = 1.17 \pm 0.02 \quad (2.12)$$

is more realistic. Within error bounds we find good agreement with the values of [14] and [12]. From the results (2.10) and (2.12) we obtain the fractal dimension  $\mu = 2.03 \pm 0.04$  using the scaling relation  $\mu = \lambda/\nu$  [14]. This does not quite agree with [14] where  $\mu = 1.96 \pm 0.01$  was found, but would favour instead the expectation  $\mu = 2$  of [13]. Unfortunately, with our simulations we had not aimed at determining  $\mu$  and we are therefore not able to clarify this interesting point.

## 2.3 Density and time evolution

Here we study the critical behaviour of the stationary density as well as the temporal behaviour of the density. The latter yields the lowest gap in the spectrum of the time-evolution operator which is given by a straightforward generalization of eq. (3.6) in [15]. Some high relaxational modes of this time-evolution operator can be written down explicitly as we demonstrate in Appendix A. In one dimension, the low-lying spectrum of this operator could be studied numerically [15], but this is not feasible in higher dimensions. Fortunately, simulations of  $\rho(t)$  exhibit much clearer features in two dimensions than was the case in one dimension. This is illustrated by Fig. 3 which shows the initial time evolution of  $\rho(t)$  after the system was started at  $\rho(0) = 1/2$ .

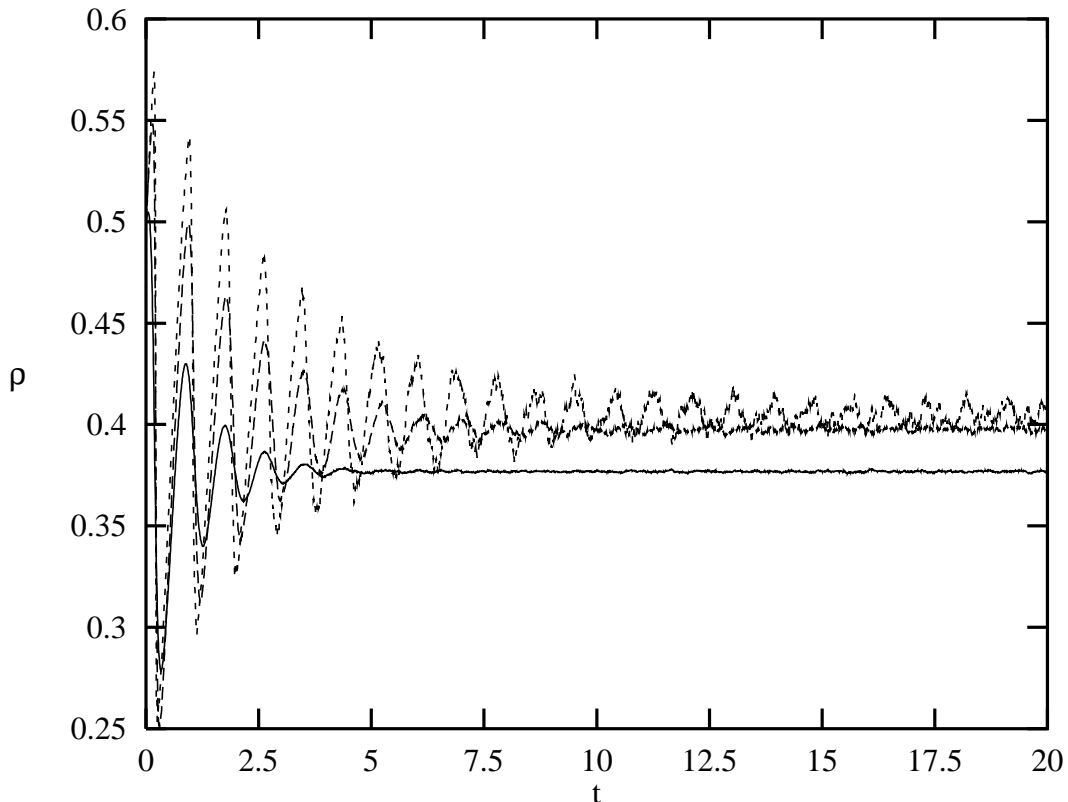


**Fig. 3:** The density  $\rho(t)$  as a function of global time  $t$ . Shown are results from simulations with  $f/p = 10^{-2}$  (bottom, full line),  $f/p = 10^{-3}$  (line with long dashes, middle) and  $f/p = 10^{-4}$  (top line with short dashes).



First we examine the critical behaviour of the stationary density of trees  $\rho(\infty)$ . The values in Table 1 are obtained by averaging  $\rho(t)$  over times  $t$  after the equilibration time, i.e. at or beyond the right border of Fig. 3.

$f/p$	$\rho(\infty)$	oscillation period $T_{\text{osc}}$	decay time $T$
$1 \cdot 10^{-2}$	0.376833	$0.878 \pm 0.028$	0.988
$7 \cdot 10^{-3}$	0.381539	$0.889 \pm 0.043$	1.155
$5 \cdot 10^{-3}$	0.385406	$0.890 \pm 0.014$	1.312
$3 \cdot 10^{-3}$	0.390296	$0.878 \pm 0.012$	1.588
$2 \cdot 10^{-3}$	0.393463	$0.883 \pm 0.017$	1.719
$1.4 \cdot 10^{-3}$	0.395793	$0.883 \pm 0.025$	1.966
$1 \cdot 10^{-3}$	0.397672	$0.879 \pm 0.026$	2.296
$7 \cdot 10^{-4}$	0.399321	$0.878 \pm 0.011$	2.455
$5 \cdot 10^{-4}$	0.400673	$0.881 \pm 0.048$	2.603
$3 \cdot 10^{-4}$	0.402291	$0.875 \pm 0.015$	3.645
$2 \cdot 10^{-4}$	0.403231	$0.876 \pm 0.026$	3.559
$1 \cdot 10^{-4}$	0.404696	$0.868 \pm 0.031$	3.951

Table 1: Estimates with  $L = 16384$  for the stationary density of trees  $\rho(\infty)$  and the lowest decay mode in  $\rho(t)$  of the two-dimensional forest-fire model.

These values are in good agreement with

$$\rho_c - \rho(\infty) \sim \left(\frac{f}{p}\right)^{1/\delta}, \quad (2.13)$$

where the critical density  $\rho_c$  and the critical exponent  $\delta$  are given by

$$\rho_c = 0.40844 \pm 0.00011, \quad (2.14)$$

$$1/\delta = 0.466 \pm 0.004. \quad (2.15)$$

These results agree within error bounds with the values obtained in [14], but our bounds are smaller. In particular we can now rule out that  $1/\delta = 1/2$  as proposed by [13].

Having determined  $\rho(\infty)$ , it is straightforward to extract the oscillation period and decay time of the slowest decay mode from  $\rho(t)$ . First, one determines those  $t$  where  $\rho(t)$  crosses the value  $\rho(\infty)$ . From the distances between these crossings the oscillation period  $T_{\text{osc}}$  can be determined easily. Averaging 10 to 15 half oscillation periods estimated in this manner for a suitable interval of time in Fig. 3 leads to the values given in Table 1. One observes that the oscillation period equals  $T_{\text{osc}} = 0.88$  within error bounds for all  $f/p$ , i.e. the slowest relaxational mode oscillates with a constant frequency. This is to be contrasted with the one-dimensional case where simulations of  $\rho(t)$  clearly demonstrated that the oscillation period depends on  $f/p$  [15].

Finally, we extract the leading decay time  $T$  from  $\rho(t)$  according to the following procedure. At times  $t$  precisely in the middle between two subsequent crossings used for the

determination of the oscillation period, the value of  $|\rho(t) - \rho(\infty)|$  is determined. One finds for these (approximately ten) values of  $t$  that  $|\rho(t) - \rho(\infty)| \sim \exp(-t/T)$  from which it is straightforward to obtain the estimates for  $T$  presented in Table 1 <sup>3)</sup>. These values for  $T$  are compatible with a critical behaviour

$$T \sim \left(\frac{f}{p}\right)^{-\zeta}, \quad (2.16)$$

where the critical exponent  $\zeta$  is determined to be

$$\zeta = 0.314 \pm 0.013. \quad (2.17)$$

This exponent probably is another new exponent that is not related to the ones determined so far [12, 14].

## 2.4 Summary of simulations

Table 2 summarizes our results for the critical exponents of the two-dimensional forest-fire model. It also includes the critical density  $\rho_c$  and the global oscillation period which seems to be independent of  $f/p$ . For comparison we have also included the results for one dimension [15, 22]. In that case, the oscillation period diverges and we have listed the exponent rather than a period in Table 2. Similarly, the amplitude  $a$  vanishes in one dimension for  $f/p \rightarrow 0$  but is roughly constant in two dimensions.

quantity	value in $d = 2$	value in $d = 1$
$\nu_T$	$0.537 \pm 0.004$	$0.8336 \pm 0.0036$
$\eta_{\text{occ}}$	0	0
$\nu$	$0.576 \pm 0.003$	1
$\eta$	$0.36 \pm 0.03$	0
$\tau$	$2.159 \pm 0.006$	2
$\lambda$	$1.17 \pm 0.02$	1
$1/\delta$	$0.466 \pm 0.004$	0
$\zeta$	$0.314 \pm 0.013$	$\approx 0.405$
$T_{\text{osc}}$	period: $0.88 \pm 0.02$	exponent $\approx 0.194$
$a$	$0.030 \pm 0.001$	$\sim (f/p)^{0.1031 \pm 0.0022}$
$\rho_c$	$0.40844 \pm 0.00011$	1

Table 2: Summary of our results for the critical behaviour of the forest-fire model.

---

<sup>3)</sup> These estimates also verify a posteriori that our equilibration times are long enough, since we have equilibrated the system for at least  $6T$  before starting to collect data. So, the non-stationary modes are damped by factors of at least  $\exp(-6) \approx 2 \cdot 10^{-3}$  during data collection.

### 3. Global models

---

We now wish to investigate to what extent one can describe the stationary properties of the two-dimensional forest-fire model by global variables in a way similar to [15]. There it was shown that in order to describe the one-dimensional critical stationary state it suffices to know the relative weight of the sum of all configurations with a fixed number of occupied (or empty) sites. Thus one is dealing with a kind of grand canonical ideal lattice gas. Such a model has no intrinsic spatial structure and leads to a two-point function independent of the distance. It can therefore be used to describe the asymptotic behaviour of the critical  $C(y)$  of Section 2. Working with the (global) density of trees  $\rho$ , one has to specify the probability distribution  $p(\rho)$  and obtains  $C(y) = \langle \rho^2 \rangle - \langle \rho \rangle^2$  for  $y \neq 0$  in the thermodynamic limit. This is positive for all continuous distributions.

In two dimensions the limits  $f/p \rightarrow 0$  and  $L \rightarrow \infty$  do not commute with each other (in contrast to one dimension). Therefore, perturbation theory cannot be used to compute  $p(\rho)$ , and in fact we do not know of a good analytic method to determine  $p(\rho)$  from the rules described in the Introduction. Therefore we use heuristic arguments and simulations to discuss it.

The forest-fire model reminds one of site percolation. Thus, it is natural to try to relate the forest-fire model to percolation and gain some insight from that. Attempts in this direction have been made e.g. in [8, 21]. We will also try to use some results of percolation theory, but we will follow a different route. Namely, we try to interpret the stationary state of the forest-fire model at the critical point as a suitable ensemble of percolation problems with a distribution  $p(\rho)$ .

It is known from percolation theory [23] that in a homogeneous configuration with a density  $\rho$  above the percolation threshold  $\rho_{\text{perc}}$  two arbitrary sites are connected with a finite probability. In such configurations, the dynamics of the forest-fire model with arbitrarily small  $f/p > 0$  would very quickly destroy all percolating clusters and thus drive the density below the percolation threshold <sup>4)</sup>. Thus, the probability  $p(\rho)$  to have a global density above the percolation threshold  $\rho_{\text{perc}}$  must vanish in the forest-fire model, i.e.  $p(\rho) = 0$  for  $\rho > \rho_{\text{perc}}$ . In one dimension one has  $\rho_{\text{perc}} = 1$  and in two dimensions  $\rho_{\text{perc}} = 0.592746$  [23]. In all simulations  $\rho(t)$  was well below this percolation threshold at all times (compare Fig. 3).

It is useful to visualize the stationary state of the forest-fire model in order to gain some intuition. Fig. 4 shows an area of  $760 \times 472$  sites at  $t = 66$  during a simulation with  $L = 16384$  and  $f/p = 10^{-4}$  (compare also Fig. 2 of [24], Fig. 1 of [14] and Fig. 6 of [13]). One observes that at a certain fixed time the system consists of rather well-defined patches with different mean density of trees. These patches are not to be confused with single forest clusters, they usually contain many such clusters. Their typical size increases as  $f/p$  becomes smaller, which reflects the divergence of correlation lengths. Looking at the time evolution of such a state <sup>5)</sup>, one observes an increase of density due to growth of trees that is constant throughout the patches and that lightning strikes essentially only the patches

---

<sup>4)</sup> This implies that the density  $\rho$  cannot be continuous at  $f/p = 0$  for  $d > 1$  and is the reason why perturbation theory cannot be used in higher dimensions.

<sup>5)</sup> On X11 platforms, such a visualization is possible with the code used for the simulations presented in this paper. This code is available on the WWW [19].

with the highest density. After a lightning has struck such a patch, a new patch with a low density is created. This new density is not really zero because there are always some trees in the patch that are not connected to the cluster which is destroyed. The idea now is that the important information about the critical stationary state is given by the distribution  $p(\rho)$  of densities in these patches and that nothing essential changes if we replace such patchy systems with an ensemble of systems of *global* density  $\rho$  occurring with the same probability  $p(\rho)$ . Of course, it remains to be tested to what extent this picture works.

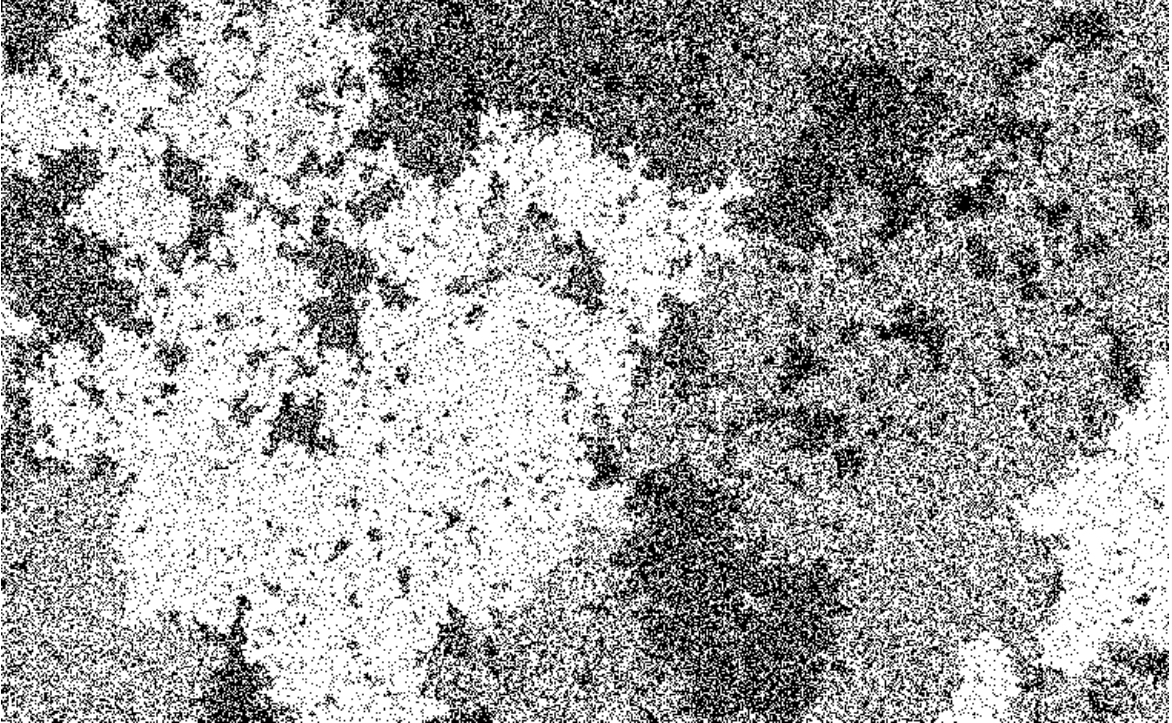


**Fig. 4:** Snapshot of an area with  $760 \times 472$  sites in the stationary state during a simulation with  $L = 16384$  and  $f/p = 10^{-4}$ . Trees are black and empty places white.

### 3.1 A simple model

Let us make a very simple model based on these ideas. Assume that below the percolation threshold  $\rho_{\text{perc}}$  trees just grow (with probability  $p = 1$ ) and no lightning strikes. As soon as the percolation threshold is exceeded, lightning strikes immediately and destroys all trees in the system. In order to determine  $p(\rho)$  we first compute the mean lifetime of a configuration with density  $\rho$ , assuming that no lightning strikes (this consideration will also be useful later on). Such a configuration lives precisely  $n$  local updates if  $n - 1$  times an occupied place and then an empty place are selected. Because of the above assumptions there is no correlation and therefore the probability of this to happen is given by  $\rho^{n-1}(1 - \rho)$ . This yields the expectation value  $t(\rho)$  of the lifetime as

$$t(\rho) = \sum_{n=1}^{\infty} n \rho^{n-1} (1 - \rho) = \frac{1}{1 - \rho}. \quad (3.1)$$

If no lightning strikes, the probability  $p(\rho)$  to find a configuration with density  $\rho$  is proportional to the lifetime of a state with this density. Taking into account that lightning

strikes all trees at  $\rho_{\text{perc}}$ , we find for this simple model

$$p(\rho) = \begin{cases} \mathcal{N}(1 - \rho)^{-1}, & \rho < \rho_{\text{perc}}, \\ 0, & \rho > \rho_{\text{perc}}, \end{cases} \quad (3.2)$$

with the normalization constant given by  $\mathcal{N}^{-1} = \int_0^{\rho_{\text{perc}}} d\rho (1 - \rho)^{-1}$ . In one dimension, (3.2) agrees with eq. (5.4) of [15] which was derived there using a different argument.

This simple model has the following periodic time evolution: Trees grows until the density reaches the percolation threshold. Then lightning strikes and the process is restarted with a completely empty system. The average time needed for such a cycle is precisely the global oscillation time and is given by  $\int_0^{\rho_{\text{perc}}} d\rho t(\rho)$ . Inserting  $t(\rho)$  according to (3.1) and the value of  $\rho_{\text{perc}}$  in two dimensions yields an oscillation period of  $T_{\text{osc}} \approx 0.898$  which is in very good agreement with what we found in simulations (compare Table 1). The mean density is given by  $\int_0^1 d\rho \rho p(\rho)$  from which one finds a critical density  $\rho_c = 0.340 \dots$  (this deviates notably from the result (2.14) found by simulations of the full model). Finally, the probability to find two trees at arbitrary places is given by the second moment of  $p(\rho)$ , i.e. by  $\int_0^1 d\rho \rho^2 p(\rho)$ . So, the two-point function exceeds the value  $\rho_c^2$  by an amount  $a = 0.0289 \dots$  which agrees within error bounds with what we found by simulations for the large-distance asymptotics of the two-point function. Cluster-type quantities are not accessible as easily and would e.g. require again Monte-Carlo simulations.

Although this simple model yields very good values for two quantities, its failure to give the correct  $\rho_c$  is not surprising. Firstly, we have neglected the fact that lightning can already strike configurations with  $\rho < \rho_{\text{perc}}$  even for arbitrarily small  $f/p > 0$  (compare Appendix A). Secondly, lightning does not really lead to the completely empty system, but usually leaves some isolated trees or small clusters in the patch behind. Unfortunately we do not know how to treat either effect analytically. This lack of knowledge also has the effect that we can in general not compute an oscillation time from  $p(\rho)$  although we do of course still think of the system as evolving in cycles (compare also section 6.3.2 of [25]).

## 3.2 Realistic distributions

Next we try to obtain a realistic  $p(\rho)$  from Monte-Carlo simulations. Measurements of the global density cannot be used to extract  $p(\rho)$  from a simulation, because  $\rho$  fluctuates only very little around its mean value for sufficiently large systems (see Fig. 3). Therefore, one has to look at the distribution of local densities. In a large system, areas with different local densities coexist and we are interested precisely in these local fluctuations and not just the global average. We have decided to divide the system into  $16 \times 16$  plaquettes and use the distribution of the average density per plaquette. This size of the plaquettes was chosen because then their linear extent is much smaller than the correlation lengths and they contain sufficiently many sites to obtain a fairly smooth distribution. Fig. 5 shows a result  $p_{\text{re}}(\rho)$  obtained in this manner using the parameter values closest to the critical point, namely  $f/p = 10^{-4}$  and  $L = 16384$ . Samples were taken at the same 90 times where also the correlation functions were determined, amounting to a total of almost  $10^8$  samples for local densities. The normalization in Fig. 5 is such that  $\sum_{r=0}^{256} p_{\text{re}}(r/256) = 1$ .

As explained above, the first and second moments of  $p(\rho)$  are related to the mean density and the asymptotic value of the two-point function. From this one finds

$$\rho(\infty) = 0.4044 \dots, \quad a = 0.031 \dots \quad (3.3)$$

The way we have determined  $p_{\text{re}}(\rho)$  ensures that the first moment indeed equals the value obtained by directly taking a global average. The slight difference between (3.3) and the value for  $\rho(\infty)$  in Table 1 is due to the fact that the latter is based on a much larger amount of configurations. As for the simple model presented before, the prediction for  $C(y) = a \approx 0.031$  agrees within error bounds with what we expect for the asymptotics of the two-point function at the critical point.

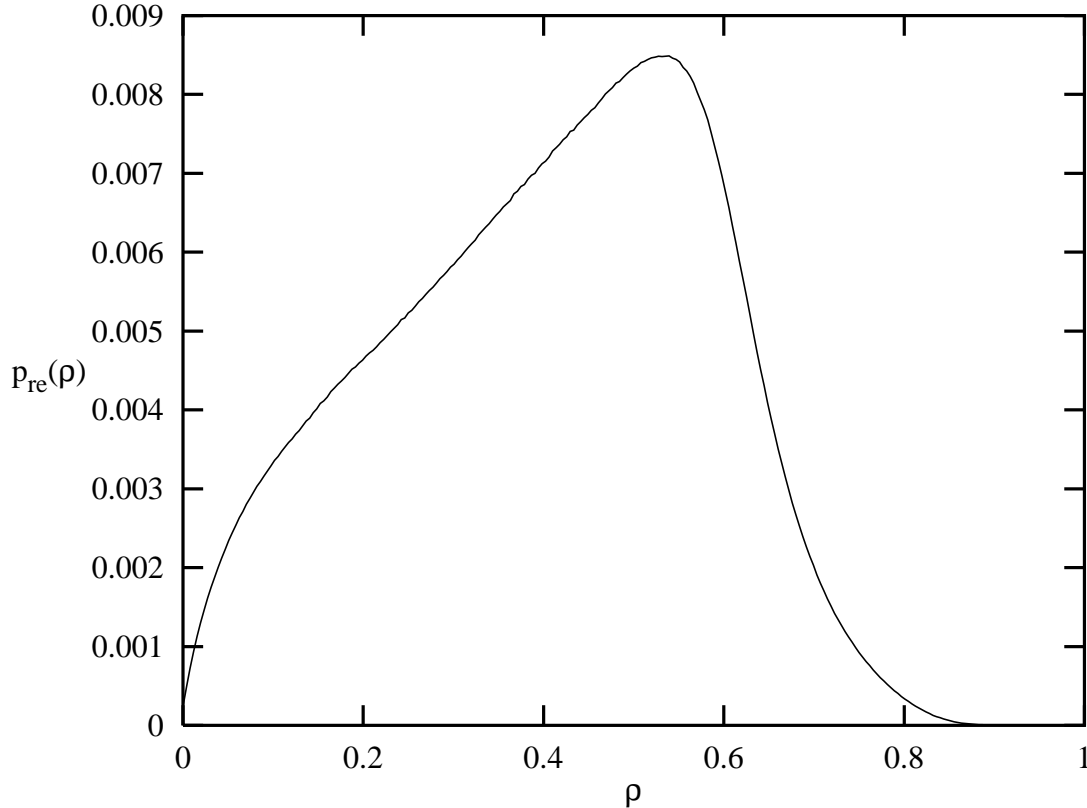


**Fig. 5:** Result for the distribution  $p_{\text{re}}(\rho)$  on  $16 \times 16$  plaquettes in a simulation with  $L = 16384$  and  $f/p = 10^{-4}$ .

Even though this basic test yields good values, one should be aware that examining the system only in windows blurs the distribution in Fig. 5 in several ways. Firstly, looking through a window containing only 256 sites, one finds a smearing of the density by  $\Delta\rho \approx 0.02$  just because of statistical effects. Secondly, such windows may accidentally intersect the boundary between two patches with low and high densities. This has the effect that  $p(\rho)$  is estimated too large for intermediate  $\rho$  and too small for the extremal ones. Our choice of  $16 \times 16$  plaquettes is designed to make both effects reasonably small and is about the best we can do.

Let us now discuss Fig. 5 keeping these effects in mind. For not too small values of  $\rho$ ,  $p_{\text{re}}(\rho)$  increases slowly and reaches a maximum around  $\rho \approx 0.54$ . Around  $\rho \approx 0.62$  there is a sharp decrease. The broad distribution shows that fluctuations of  $\rho$  are important. A peak just below the percolation threshold  $\rho_{\text{perc}}$  and a steep decrease above it correspond to our expectation. However, there is still a substantial contribution to  $p_{\text{re}}(\rho)$  above  $\rho_{\text{perc}}$  which is not explained by windowing effects. This is due to the patchy structure of the system: Finite patches with  $\rho > \rho_{\text{perc}}$  are not destroyed instantly, but rather live for a time which is the longer the smaller these patches actually are. One could also say that the

patchy structure demonstrates that the system is actually correlated. In particular at small distances ( $y \lesssim 20$ ), the two-point function  $C(y)$  retains a  $y$ -dependence (compare Section 2.1) for  $f/p \rightarrow 0$  and thereby exceeds the asymptotic constant  $a$ . This correlation is necessary to observe a non-trivial distribution of local densities, but also leads to contributions to  $p(\rho)$  above the percolation threshold.

So, if we want to work with a ‘realistic’  $p(\rho)$ , the best we can do is to proceed with the one shown in Fig. 5. Alternatively, one can work with an approximation to this distribution where one suppresses the undesired  $p(\rho)$  above the percolation threshold by hand. One such approximation we have examined is a linear one, i.e  $p_{\text{lin}}(\rho) \sim \rho$  for  $\rho < 0.59$  and  $p_{\text{lin}}(\rho) = 0$  for  $\rho > 0.59$ . This linear distribution yields  $\rho_c \approx 0.395$  and  $a \approx 0.019$  (both somewhat too small).

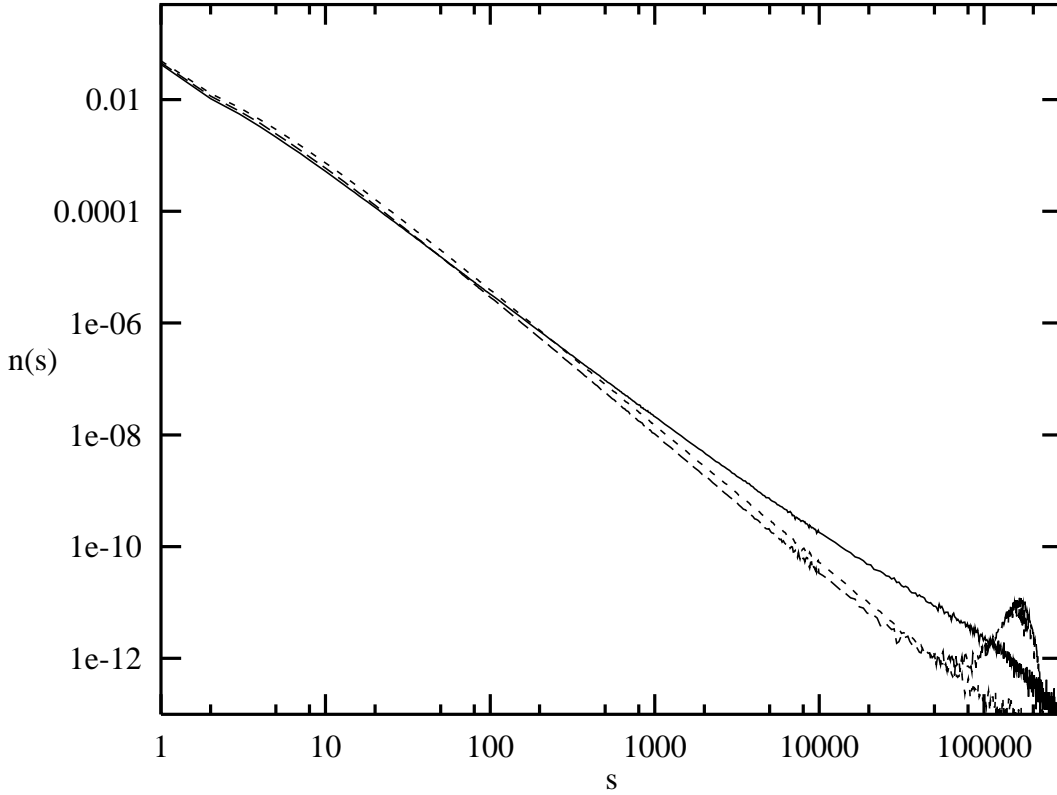


**Fig. 6:** The cluster-size distribution obtained from a simulation of the full model with  $L = 16384$  and  $f/p = 10^{-4}$  (full line), the one based on  $p_{\text{re}}(\rho)$  (long dashes) and the result obtained from  $p_{\text{lin}}(\rho)$  (short dashes).

The determination of the cluster distribution  $n(s)$  and  $K(y)$  is a complicated combinatorial problem which we solve again using simulations. One creates configurations with densities distributed according to the given  $p(\rho)$  and then measures  $n(s)$  and  $K(y)$ . We have created 100000 configurations on a  $512 \times 512$  lattice distributed according to  $p_{\text{re}}(\rho)$  and 70000 configurations on a  $1024 \times 1024$  lattice for  $p_{\text{lin}}(\rho)$ . Fig. 6 shows the cluster-size distribution  $n(s)$  obtained in this manner together with the one obtained from a simulation of the full model. For small cluster sizes ( $s < 100$ ), all three distributions are close to each other. However, at larger  $s$  the distributions based on a globally given  $p(\rho)$  decay faster than the true  $n(s)$ . The corresponding exponent is  $\tau \approx 2.48$  for the distribution  $p_{\text{re}}(\rho)$  and  $\tau \approx 2.44$  for  $p_{\text{lin}}(\rho)$  – both much closer to the mean-field value  $\tau = 5/2$  [21] than to the true value

(2.11). In Fig. 6 one also observes a peak in the cluster-size distribution corresponding to  $p_{\text{re}}(\rho)$  for  $1 \cdot 10^5 \leq s \leq 2.5 \cdot 10^5 \approx 512^2$ , i.e. just below the volume of the system. This is due to the non-vanishing of  $p_{\text{re}}(\rho)$  for  $\rho > \rho_{\text{perc}}$  which leads to clusters spanning a finite (and large) fraction of the system.

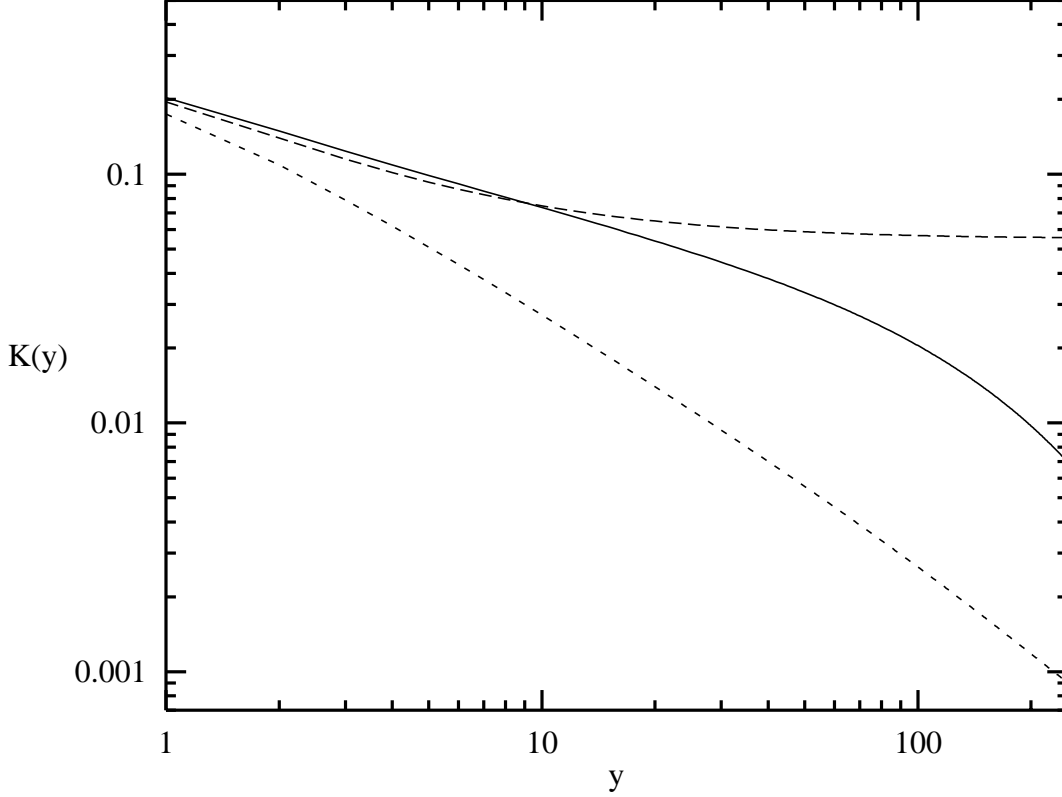


**Fig. 7:** The full line shows the correlation function  $K(y)$  obtained from a simulation of the full model with  $L = 16384$  and  $f/p = 10^{-4}$ . The result for  $p_{\text{re}}(\rho)$  is shown by the line with long dashes, the one obtained from  $p_{\text{lin}}(\rho)$  is indicated by the shorter dashes.

Fig. 7 shows the probability  $K(y)$  to find two trees at distance  $y$  inside the same cluster. Here, the results obtained from the two  $p(\rho)$ 's deviate more notably from the result obtained by simulation of the full model (full line). As noted above, the distribution  $p_{\text{re}}(\rho)$  gives rise to percolating clusters and produces a constant background in  $K(y)$  of approximately 0.0552. After subtracting this background, one can fit  $K(y)$  with (2.8) for  $\xi_c \approx 180$  and  $\eta \approx 0.92$ . This value for  $\eta$  is more than twice as large the true one (2.9). For  $p_{\text{lin}}(\rho)$  one finds good agreement with the form (2.8) for  $\xi_c = L/2$  and  $\eta \approx 0.95$ .

### 3.3 Summary and outlook on global models

We have shown that the distributions  $p_{\text{re}}$  and  $p_{\text{lin}}$  lead to a power law for  $n(s)$ . One can check that the same is true for other  $p(\rho)$ 's that are cut off at  $\rho_{\text{perc}}$  in a way similar to  $p_{\text{lin}}$ . Thus, a power law in  $n(s)$  arises automatically from a description in terms of global quantities and need not be a signal for criticality in a conventional sense. However, in all examples for  $p(\rho)$  discussed so far, we obtained values for  $\tau$  and  $\eta$  that are unsatisfactorily larger than those of the full model. Nevertheless, a description in terms of  $p(\rho)$  can still be forced to work because for two-dimensional critical percolation one has  $\tau \approx 2.055$  and



$\eta \approx 0.208$  [23] – values which are smaller than the ones in Table 2. So, one can obtain the desired value e.g. of  $\tau$  by peaking the distribution  $p(\rho)$  more prominently just below  $\rho_{\text{perc}}$ . Adjusting just  $\tau$  to its correct value can be expected to also give a reasonably good approximation for  $\eta$ . Afterwards, both  $\rho_c$  and  $a$  may be tuned to the desired values by adding another peak in  $p(\rho)$  for smaller densities (which does not contribute to large clusters and thus affect the asymptotics of cluster quantities). However, there does not seem to be a natural way to make these adjustments. In particular, local densities above  $\rho_{\text{perc}}$  do exist in the full model which would have to be discarded by hand in a global model in order to obtain the correct  $K(y)$ .

In one dimension the spatial structure becomes irrelevant at the critical point [15]. We have seen in this Section that this can be generalized to the qualitative features of the critical correlations in two dimensions, but not to the quantitative details. In contrast to the one-dimensional case we had no analytical tools at our disposal and have therefore not been able to derive the distribution  $p(\rho)$  of local densities explicitly. The introduction of block-spin variables is reminiscent of real-space renormalization group ideas and it would be interesting to see if they can be used to find  $p(\rho)$ . However, one would have to go beyond the block-spin renormalization-group study of [18]. Firstly, one would have to admit densities different from 0 or 1 for the block-spin variables, and moreover the dynamics should not be treated just in mean-field approximation.

Two-dimensional percolation is believed to be conformally invariant (see e.g. [26]). The globalized models are just ensembles of percolation problems and should therefore be conformally invariant as well. It would be interesting to know if also the stationary state of the full model in two space dimensions is conformally invariant, even if the standard techniques of conformal field theory would probably not say much about quantities like cluster sizes.

## 4. Conclusions

---

In this paper we have again looked at several aspects of the two-dimensional forest-fire model. Firstly, we have shown that the two length scales  $\xi$  and  $\xi_c$  have different critical exponents. That this might be possible had been suggested by a study of the one-dimensional model [15] which illustrates that one-dimensional systems can provide useful insights because of their relative simplicity even if one is actually interested in higher-dimensional versions. This result shows that in generic non-equilibrium systems geometric objects and the usual (occupancy) correlation functions can behave completely differently. For an equilibrium system as the Ising model such an observation was already made some time ago in [27]. In this case, percolation occurs away from the critical point, i.e. the two length scales are so different that they diverge at different temperatures (see e.g. [28, 23]).

In order to show that  $\nu_T \neq \nu$  we had to improve the error bounds of earlier investigations. As a by-product we have also improved the accuracy of other critical exponents. It may be possible that one could still improve the error bounds by another digit using optimized code on today's most powerful computers. Historically, Monte-Carlo simulations have already several times lead to values for the critical exponents that had to be corrected later on [8, 12, 13, 14] and as we have shown here, some of them were still not treated adequately. Therefore, it may be desirable to perform yet another independent verification of the results presented here, but a further increase of accuracy may not be necessary for this end.

The second part of the paper focussed on a globalized model. We found that one can easily obtain power laws in the cluster-size distribution by discarding the spatial structure, i.e. by making the usual two-point function independent of the spatial coordinates. This generalizes a result obtained for one dimension in a previous paper [15] and is line with the observation in [16], based on a different one-dimensional model, that one can obtain power laws in clusters or avalanches by global (‘coherent’) driving. However, some quantitative predictions of the globalized model did not work out satisfactorily. One reason is that the full two-dimensional forest-fire model has non-trivial two-point functions at least at small distances which is also reflected by the existence of patches with local densities above the percolation threshold. In addition, the full model exhibits many critical exponents that cannot be described by a global model.

A study of the usual correlation functions would also be desirable in other models of self-organized criticality where they have not yet been investigated. This could help to clarify to what extent the process of self-organization can be regarded as a global phenomenon. Two-point correlation functions would also be important quantities to examine in experiments. It would e.g. be interesting to extract the spatial correlation functions of the local heights and slopes from the experimental data of [3].

Even for the two-dimensional forest-fire model there are still many issues we have not looked at, including e.g. finite-size effects. We have only looked at the regime  $fV \gg p$  which is close to the thermodynamic limit. One could also look at a different limit, namely  $fV \ll p$  where the first-order approximation of [15] applies independent of the spatial dimension. In this limit, trees grow until the lattice is full and after a certain time of rest, lightning destroys all these trees and the process starts again. It would be interesting to see how this behaviour crosses over to the critical behaviour studied here as the volume of the system is increased, and if finite-size scaling can be observed.

## Acknowledgments

---

Useful discussions with S. Clar are gratefully acknowledged. The work of A.H. has been funded by the Deutsche Forschungsgemeinschaft.

## Appendix A. Some exact relaxational modes

---

The time-evolution operator for the forest-fire model in general dimensions  $d$  can be written down along the lines of Section 3 of [15]. Then one can obtain *exact* excited states using the same argument as at the end of Section 3 of [15] (cf. in particular eq. (3.15) loc. cit.).

The crucial step is to consider a class of configurations that contain a single cluster of trees and where each empty place is a neighbour of a tree. The last condition means that the configuration still consists of a single cluster if a tree is grown at any of the empty places. Now we consider states that are built out of such a configuration but have non-zero momentum  $\vec{P} \neq \vec{0}$ . Lightning strokes in such configurations lead to the completely empty system. In states with  $\vec{P} \neq \vec{0}$  the completely empty system is reached by lightning with coefficients that contain a sum over all roots of unity such that lightning maps states constructed in this manner to zero. Thus, the only terms in the image come from growing

a single tree in a configuration. Now, as in eq. (3.15) of [15] one can write down eigenvalue equations that are upper triangular in the number of empty places  $N$ . The diagonal terms in these equations are already the eigenvalues

$$\Lambda_N = Np + f/p(V - N). \quad (\text{A.1})$$

One must have  $N \geq 1$  because the completely full system cannot be used to build a state with non-zero momentum.

The number of empty places  $N$  is restricted by the above conditions. For  $d = 1$  only the two configurations considered in [15] meet the requirement of consisting of a single cluster and remaining in this class after growing an arbitrary tree. Thus,  $N \leq 2$  for  $d = 1$ , and the density  $\rho$  of these two configurations tends to 1 in the thermodynamic limit.

For general  $d$  note first that the connectedness of the cluster implies that the trees must form at least one-dimensional objects. This is most efficiently implemented by grouping the trees in straight lines. In the hyperplane perpendicular to these lines, a tree can have  $2d - 2$  empty places as neighbours. Thus, at least one place out of  $2d - 1$  must be occupied by trees in order to meet the requirements. This yields  $N \lesssim V(1 - 1/(2d - 1))$ . Equivalently, all configurations containing only a single cluster that retain this property after growing a tree must have  $\rho \geq 1/(2d - 1)$ . For  $d \leq 3$  we can indeed specify configurations that saturate this lower bound. In  $d = 1$  this limit is  $\rho = 1$  and corresponds to the thermodynamic limit of an almost full system. In  $d = 2$  a configuration with  $\rho = 1/3$  is given by lines of trees that are mutually separated by two lines of empty places. The lower bound  $\rho = 1/5$  in  $d = 3$  is saturated by arranging the lines in such a way that their mutual position in the perpendicular plane corresponds to the moves of a pawn in the game of chess. Of course, the lines have to be connected by a  $d - 1$  dimensional object, but this does not change the value of  $\rho$  in the thermodynamic limit.

## References

---

- [1] P. Bak, C. Tang, K. Wiesenfeld, *Self-Organized Criticality: An Explanation of 1/f Noise*, Phys. Rev. Lett. **59** (1987) 381-384
- [2] P. Bak, C. Tang, K. Wiesenfeld, *Self-Organized Criticality*, Phys. Rev. **A38** (1988) 364-374
- [3] V. Frette, K. Christensen, A. Malthe-Sørenssen, J. Feder, T. Jøssang, P. Meakin, *Avalanche Dynamics in a Pile of Rice*, nature **379** (1996) 49-52
- [4] P. Bak, K. Sneppen, *Punctuated Equilibrium and Criticality in a Simple Model of Evolution*, Phys. Rev. Lett. **71** (1993) 4083-4086
- [5] P. Bak, H. Flyvbjerg, K. Sneppen, *Mean Field Theory for a Simple Model of Evolution*, Phys. Rev. Lett. **71** (1993) 4087-4090
- [6] M. Paczuski, S. Maslov, P. Bak, *Avalanche Dynamics in Evolution, Growth, and Depinning Models*, Phys. Rev. **E53** (1996) 414-443
- [7] C.L. Henley, *Self-Organized Percolation: A Simpler Model*, Bull. Am. Phys. Soc. **34** (1989) 838

- [8] B. Drossel, F. Schwabl, *Self-Organized Critical Forest-Fire Model*, Phys. Rev. Lett. **69** (1992) 1629-1632
- [9] P. Bak, K. Chen, C. Tang, *A Forest-Fire Model and Some Thoughts on Turbulence*, Phys. Lett. **A147** (1990) 297-300
- [10] P. Grassberger, H. Kantz, *On a Forest Fire Model with Supposed Self-Organized Criticality*, J. Stat. Phys. **63** (1991) 685-700
- [11] B. Drossel, W.K. Moßner, F. Schwabl, *Computer Simulations of the Forest-Fire Model*, Physica **A190** (1992) 205-217
- [12] C.L. Henley, *Statics of a "Self-Organized" Percolation Model*, Phys. Rev. Lett. **71** (1993) 2741-2744
- [13] P. Grassberger, *On a Self-Organized Critical Forest-Fire Model*, J. Phys. A: Math. Gen. **26** (1993) 2081-2089
- [14] S. Clar, B. Drossel, F. Schwabl, *Scaling Laws and Simulation Results for the Self-Organized Critical Forest-Fire Model*, Phys. Rev. **E50** (1994) 1009-1018
- [15] A. Honecker, I. Peschel, *Critical Properties of the One-Dimensional Forest-Fire Model*, Physica **A229** (1996) 478-500
- [16] M.E.J. Newman, K. Sneppen, *Avalanches, Scaling and Coherent Noise*, preprint cond-mat/9606066, CTC96TR237
- [17] J. de Boer, A.D. Jackson, T. Wettig, *Criticality in Simple Models of Evolution*, Phys. Rev. **E51** (1995) 1059-1074
- [18] V. Loreto, A. Vespignani, S. Zapperi, *Renormalization Scheme for Forest-Fire Models*, J. Phys. A: Math. Gen. **29** (1996) 2981-3004
- [19] <http://www.physik.fu-berlin.de/~ag-peschel/software/forest2d.html>
- [20] S. Clar, private communication
- [21] K. Christensen, H. Flyvbjerg, Z. Olami, *Self-Organized Critical Forest-Fire Model: Mean-Field Theory and Simulation Results in 1 to 6 Dimensions*, Phys. Rev. Lett. **71** (1993) 2737-2740
- [22] S. Clar, B. Drossel, F. Schwabl, *Exact Results for the One-Dimensional Self-Organized Critical Forest-Fire Model*, Phys. Rev. Lett. **71** (1993) 3739-3742
- [23] D. Stauffer, A. Aharony, *Perkolationstheorie, Eine Einführung*, VCH Weinheim (1995) (German translation of *Introduction to Percolation Theory*, Taylor & Francis London (1992))
- [24] B. Drossel, F. Schwabl, *Self Organization in a Forest-Fire Model*, Fractals **1** (1993) 1022-1029
- [25] B. Drossel, *Strukturbildung in offenen Systemen*, Ph.D. thesis, München (1994)
- [26] R. Langlands, P. Pouliot, Y. Saint-Aubin, *Conformal Invariance in Two-Dimensional Percolation*, Bull. Am. Math. Soc. **30** (1994) 1-61
- [27] H. Müller-Krumbhaar, *The Droplet Model in Three Dimensions: Monte Carlo Calculation Results*, Phys. Lett. **A48** (1974) 459-460
- [28] J.L. Cambier, M. Nauenberg, *Distribution of Fractal Clusters and Scaling in the Ising Model*, Phys. Rev. **B34** (1986) 8071-8079